The Erratic Emission of Pyrene on Gold Nanoparticles

Gionata Battistini, Pier Giorgio Cozzi, Jukka-Pekka Jalkanen, Marco Montalti,* Luca Prodi, Nelsi Zaccheroni, and Francesco Zerbetto*

Dipartimento di Chimica "G. Ciamician", Università di Bologna, Via Selmi 2, I-40126 Bologna, Italy

ABSTRACT Gold nanoparticles functionalized with chromophores are known to present unpredictable fluorescence as a function of their structure. Odd–even effects, based on the number of methylene units of the chain to which the fluorophore is attached, and the nature of the anchoring group on the gold surface have, in the past, been suggested to be responsible for the behavior. Here we investigate the fluorescence processes of two newly synthesized pyrene derivatives bound to gold nanoparticles. Two structurally identical ligands, differing only in the nature of the anchoring group (a thiolate in one case and an amine in the other), were newly synthetized and attached to the gold nanoparticles. The same changes in the fluorescence properties, namely, a red spectral shift with a moderate increase of the quantum yield and a shortening of the excited-state lifetime, are observed in the two cases and ascribed to the proximity of the gold core. By comparison with the results reported for other pyrene derivatives, it has been possible to draw the conclusions that (i) the nature of the binding group does not affect the fluorescence properties of the fluorophores attached to the nanoparticle surface and (ii) much stronger fluorescence is observed in the case of pyrene separated from the gold by short alkyl chain. The unusual behavior is explained in simple terms of competing chain—chain and chromophore–chromophore interactions and by means of proper energy diagrams.

KEYWORDS: gold nanoparticles · fluorescence enhancement · pyrene · competing interactions · electron transfer

The integration of molecular systems with the unusual properties of gold nanoparticles (NPs) is the focus of a concerted effort directed toward achieving the control and the improvement of the properties of a wide range of electro-, photo-, or bioactive molecules.[1–17] The two-fold intent is to understand the interactions between NPs and the active systems and to design new functional materials that owe their properties to the proximity of a molecule to the metal surface. An example is the possibility to activate or deactivate the photophysical properties of a chromophore by a NP core.[18–37] The presence of gold nanoparticles can effectively quench fluorescence of organic molecules via energy transfer mechanisms.[18–30] This distance-dependent process has been interpreted by different models.[18–22] In particular, small NPs with a diameter of 1.4–1.5 nm do not show a coherent surface plasmon resonance and display a higher quenching efficiency than organic quenchers.[23,28–30] The rates of energy transfer have an r^{-4} distance dependence, which is compatible with the NSET (nanosurface energy transfer) theory.[28–30] Larger NPs, with a diameter of ~80 nm, enhancing the local electric fields, give increased excitation rates and also provoke faster radiative deactivation processes.[22] The phenomena are not limited to gold NPs, and several examples of fluorescence enhancement have recently been reported also for silver nanostructures and nanoparticles.[31–37]

The interplay between quenching and higher transition rates was shown by Novotny and co-workers to generate a continuous range of cases from fluorescence quenching to a fluorescent enhancement regime.[31] The quenching via energy transfer is not ubiquitous; cyanine dyes in the proximity of 12 nm gold NPs have a fluorescence quantum yield governed directly by the radiative rate[22] and not by energy transfer in contrast with the popular Gersten—Nitzan model.[19]

A particularly low efficiency of the energy transfer process was also reported by Thomas and Kamat for 1-methylaminopyrene, see **A** in Scheme 1, bound to 5–8 nm gold nanoparticles.[38] This result is particularly significant since, to the best of our knowledge, it is the only example of a fluorophore with a very strong fluorescence when located in close proximity to a gold nanosurface.

It is intriguing that the same authors reported strong quenching of luminescence for another pyrene derivative bound to gold NPs (2–3 nm of diameter) through a longer chain, see **B** in Scheme 1.[39] In this system, the excited-state deactivation takes place mainly by injection of electrons into the

*Address correspondence to marco.montalti2@unibo.it.

Received for review September 19, 2007 and accepted November 30, 2007.

Published online December 22, 2007.
10.1021/nn700241w CCC: $40.75

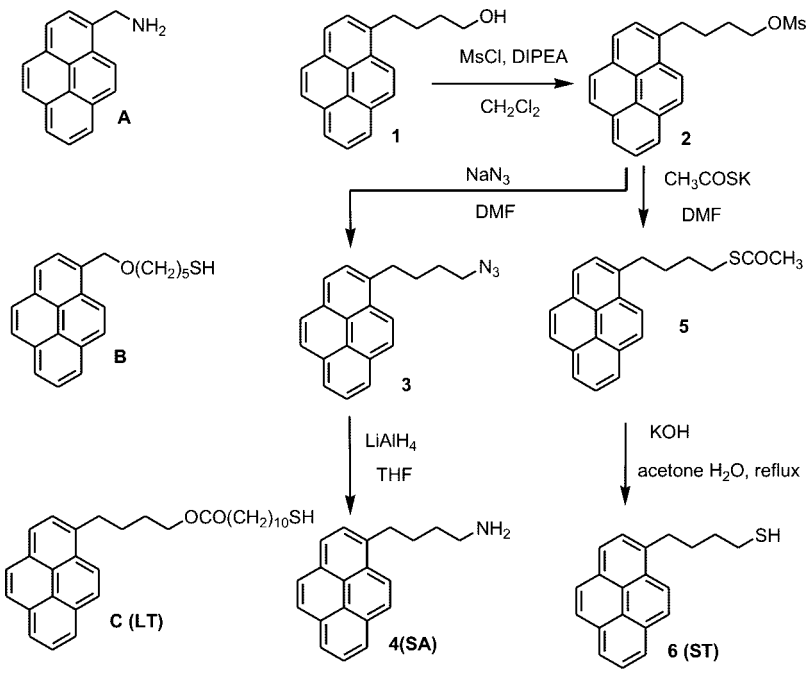

Scheme 1. Structures and synthetic procedures of the studied pyrene derivatives.

metal core with subsequent formation of a pyrenium radical cation. The dominance of the electron transfer process was confirmed by restoring the fluorescence in the presence of an electrochemical bias that prevented the occurrence of charge transfer.[40] It is perhaps puzzling that electron transfer does not take place in the case of **A**, despite the fact that the fluorophore is much closer to the NP core than in the case of **B**. The authors ascribed the different behavior to the different nature of the binding groups. The amine group of **A** was thought to polarize the gold core and prevent electron injection from the electronically excited pyrene. However, because of the structural difference between **A** and **B**, the effect could not be separated from other factors, such as distance and orientation of the fluorophores.

In this paper, we investigate the photophysical properties of two gold NPs that are functionalized with structurally similar pyrene derivatives, which are linked to the metal via short, identical alkyl chains that were newly synthesized for this work.[38–48] Compound **4**, Scheme 1, is terminated by an SH group; compound **6**, Scheme 1, is terminated by an NH_2 group. The length of the alkyl chain is long enough to prevent quenching of the excited state of pyrene via electron transfer from the amino group (see below). This undesired process would differentiate the intrinsic behavior of the amine compound from that of the correspondent thiolate. The chain is also short enough to allow the investigation of the short-range interactions between pyrene and gold. The results are also compared with the photophysical properties of NPs characterized by a larger separation between fluorophore and metal core (*viz.*, compound **C**, Scheme 1).[41,42]

RESULTS AND DISCUSSION

The Free Fluorophores. The pyrene derivatives **4** (short chain amino terminated, or **SA**), **6** (short chain thiol terminated, or **ST**), and **D** (very short chain, reference system, unable to bind to gold) have almost identical photophysical properties.[49] The absorption spectra present the typical vibrational structure of this family of fluorophores with a maximum in the lowest energy band at 343 nm ($\epsilon = 40\,000\ M^{-1}\ cm^{-1}$). In aerated THF solution, the lifetimes of the first singlet excited state measured by time-correlated single-photon counting (TCSPC) were the same, $\tau = 16$ ns, within experimental error. The similarity of the photophysical properties of the three compounds is confirmed by the perfect matching of the fluorescence spectra and the identical values of the quantum yields ($\Phi = 0.071$). These results indicate the absence of interactions between pyrene and the amino or thiolic groups, both in the ground and in the excited state, and are of particular relevance in the case of compound **4** (**SA**) where the amino group might have quenched the excited state of pyrene via electron transfer. The absence of such a process was confirmed by titration of such compound with trifluoromethanesulfonic acid: no changes in the photophysical properties of the pyrene derivative were observed upon addition of up to three equivalents of acid. In the case of an amino derivative with a shorter alkyl chain, in contrast, strong quenching of the fluorescence of the excited pyrene moieties was observed.[38] This point is fundamental when comparing the effect of binding compounds **4** (**SA**) and **6** (**ST**) to gold since there is no indirect effect caused by the modification of the interaction of the fluorophore with the linking group.

Fluorophore and NP Interactions. Nanoparticle−pyrene interactions of **4** (**SA**), **6** (**ST**) and **D** (**reference**) were investigated in three THF solutions where the molecules had the same concentration (3×10^{-6} M) and the same amount of NPs was added. The fluorescence spectra are reported in Figure 1, while the excitation spectra are shown in Figure 2. Addition of gold nanoparticles causes a strong filter effect both on the excitation and on the emission of the pyrene, and for this reason, spectral correction was required.[50,51]

The Reference System. The corrected fluorescence and excitation spectra of **D** were almost unaffected by the presence of the gold nanoparticles, which indicates a total absence of interactions. This is in agreement with the fact that **D** does not bind to the gold surface and cannot, when excited, interact with the gold NPs because of the low concentration conditions.[50,51] The lack of any interaction, even in the ground state, is also corroborated by the absorption spectrum, which is simply

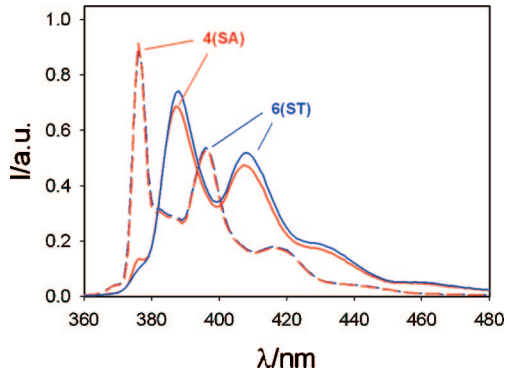

Figure 1. Corrected fluorescence spectra upon excitation at 340 nm of 4 (SA) and 6 (ST) before (– – –) and after (—) binding to gold nanoparticles.

the sum of the spectrum of **D** and that of the gold NPs; on the other hand, the absence of interaction in the excited state is further confirmed by the excited-state lifetime measurement (τ = 16 ns).

The Short-Chain System. The situation is completely different for **4** and **6**, which, however, show the same trends. The structured absorption bands of pyrene are strongly perturbed, while the Au plasmon resonance band at 520 is hardly affected, see Figure 3. Spectral deconvolution of the pyrene bands shows a reduction of the absorption to around 30% of that observed in the absence of gold. Upon binding to the NP, the fluorescence red-shifts and the vibrational structure markedly changes, as can be seen in Figures 1 and 2. The variations indicate the existence of a strong interaction between pyrene and gold, as was already observed for other similar systems.[52]

The fluorescence quantum yield increases by a factor 1.5 for **4** (**SA**) and 1.4 for **6** (**ST**) upon their binding to the gold nanoparticles. This is concomitant with a shortening of the excited-state lifetime in the case of both the amino and the mercapto derivative (τ = 6.2 and 5.7 ns, respectively). Such a behavior is not unusual for a fluorophore in the proximity of metal nanostructures and is due to an increase of the radiative constant of the fluorescent excited state.[7]

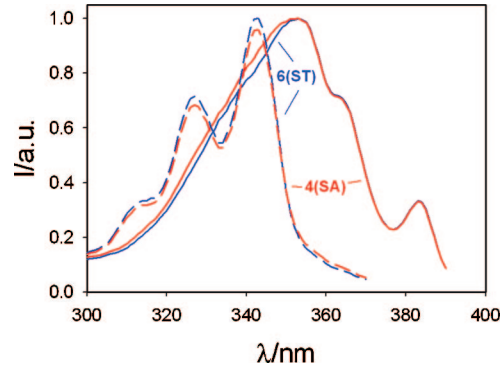

Figure 2. Corrected excitation spectra at 420 nm of 4 (SA) and 6 (ST) before (– – –) and after (—) binding to gold nanoparticles.

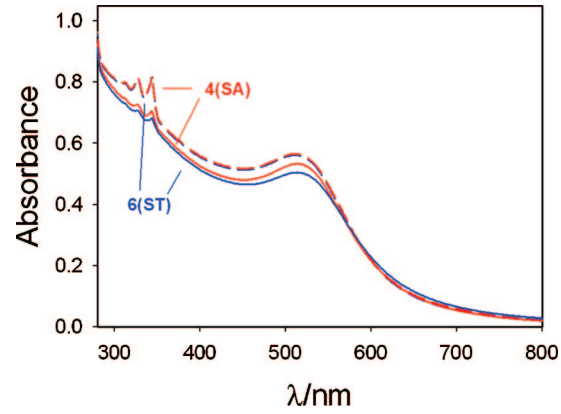

Figure 3. Absorption spectra of 4 (SA) and 6 (ST) and after binding to gold nanoparticles (—). Dashed lines represent the spectra calculated in the case of no interaction.

These results are surprising when compared with those obtained for thiol **C**(long chain thiol terminated, or **LT**; see Table 1). In fact, in the presence of the longer alkyl chain, a strong quenching (less than 10% of residual fluorescence), a slight blue shift of the fluorescence band, and a dramatic shortening of the lifetime (τ = 0.5 ns) were observed upon binding to the gold nanoparticles.

In short, we observed the reduction of the quenching efficiency of the NP when the distance is reduced, a behavior that would be extremely unusual for an energy transfer process[18–22] but that can be explained when it is considered that, in the case of pyrene, the quenching is mostly due to electron transfer processes (see below).[39]

Computational Modeling. Computational modeling can assist the unraveling of the unexpected trend of quenching with the chain length. Molecular mechanics minimizations were performed for a system with 25 pyrene chains on Au(111). The pyrenes were attached to the surface via chains of length of 4 and 11 carbon atoms, C4 and C11. In the optimized geometries, for the short chain, the tilt angle with respect to the normal to the metal surface was ~20°. This value is about half as large as that calculated for the more flexible and longer chains, where it increases to 45–48°. The origin of the effect is readily explained. When the chains are short, the dominant interaction that governs the packing of the organic layer is between the pyrene moieties. Because of the short chain length, the chain–chain interaction is small and the molecules arrange themselves to

TABLE 1. Effect of the Binding to Gold NP on the Fluorescence Properties

compound	chain	binding group	shift[a]	quenching[a]
A[b]	C_1	$-NH_2$	red	No
4 (SA)	C_4	$-NH_2$	red	No
6 (ST)	C_4	-SH	red	No
C (LT)[c]	C_{11}	-SH	blue	Yes

[a]After binding to gold NP with respect to the free ligands. [b]Data from ref 8. [c]Data from ref 8.

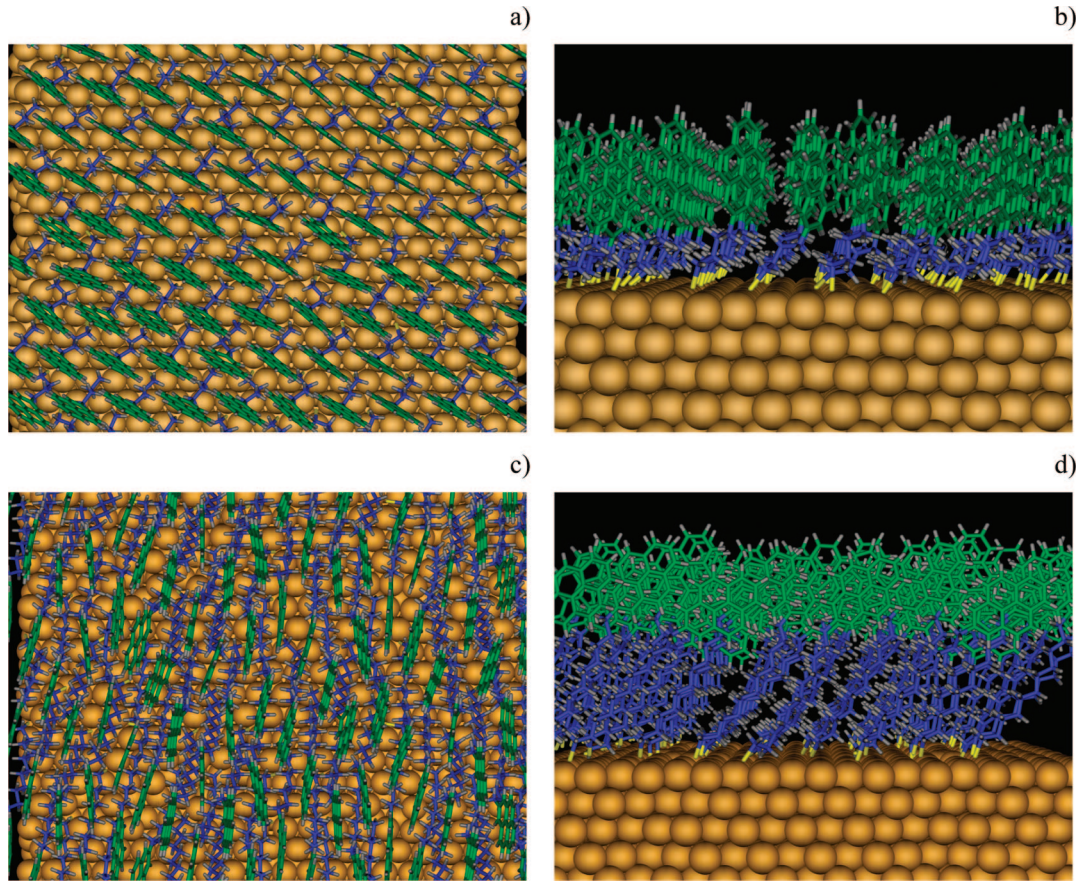

Figure 4. Top and side views of optimized monolayers: (a, b) the short C4 chain; (c, d) the long C11 chain. The alkane chain is blue, and pyrene is green.

maximize pyrene−pyrene interactions.[12] When the chains elongate, the chain−chain interactions become more important and the molecules arrange themselves accordingly.

The difference in tilt angle of the two types of chains has an important consequence: for the short C4 chains, the pyrene fluorophore is almost perpendicular to the gold surface, see Figure 4, while for the longer C11 chains, pyrene lies flatter with respect to the metal surface.

The electronic interactions between the gold core and the pyrene layer are driven by their relative geometrical arrangements and occur in two general ways. The first is through the overlap of the wave functions of the two fragments. The second is mediated by perturbations, such as an electric field. An example of the former is the charge transfer between metal and organic components, where the probability of the transfer is proportional to the overlap of the electronic clouds. An example of the latter is the effect of the electric field generated by the metal on the electronic states of pyrene.

The flatter orientation of the molecule, as in the case of C11, increases the probability of charge transfer, which would be zero for a perpendicular standing pyrene. Instead, the shorter distance between the fluorophore and the gold atoms, as in the case of C4, perturbs the "symmetry-allowed" electronic states via $\vec{E} \cdot \vec{\mu}$ where $\vec{\mu}$ is the transition dipole moment between the states perturbed and $\vec{E}$ is the electric field generated by the metal core. In other systems, we found that the electric field generated by gold can be substantial and as large as 7 MV/cm.[13]

It is of interest to assess further the role of charge transfer in the short- and the long-chain systems. High-level quantum chemical calculations on the systems of Figure 4 are not feasible because of their size. To obtain a qualitative understanding, we decided to investigate, using density functional theory calculations at the B3LYP/6-31G* level, the effect on the ionization potential of the charges of the metal atoms that are present in the vicinity of an individual fluorophore. In the absence of the charges, the calculated energy difference between neutral and cationic pyrene is consistently 6.95 eV for the C4 and C11 systems. The charges of the metal atoms, calculated by the model used to optimize the geometries, are positive and must increase the ionization potential. When they are added, it was found that the ionization potential of pyrene grows to 18.66 eV for C4, while in the case of C11 it is 15.09 eV.

These values do not have a direct experimental counterpart. However, they indicate that charge transfer should be easier (and therefore there should be a larger quenching) in the case of the C11 chain.

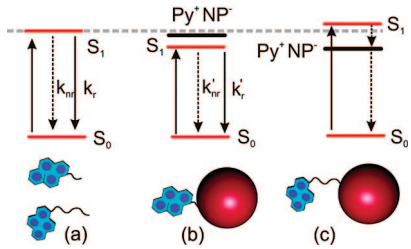

Scheme 2. Schematic representation of the photophysical processes involving the pyrene ligands. The free fluorophores show the same behaviour independently on the chain length and terminal group (a). In contrast, after binding to the nanoparticles, the energies of the fluorescent and charge transfer states depend on the chain length: case (b) is for the short chain (compounds 4 (SA), 6 (ST)); case (c) is for the long chain (compound C (LT)).

Scheme 2 shows a model that summarizes the observations. For the longer chain, the metal core generates an electric field that affects the energy levels that are accessible via the dipole moment transition of the electric field of the light. For the shorter chain, the orientation of the pyrenes lowers the charge transfer states that are energetically accessible after electronic excitation.

CONCLUSIONS

Investigation of the photophysical properties of gold nanoparticles functionalized with "short" chain compounds **4** and **6** showed, to our surprise, a counterintuitive enhancement of the fluorescence efficiency of the pyrene moieties after their binding to the gold core, while quenching was reported in the case of the "long chain" derivative **C** and for other pyrene derivatives.[49] We have demonstrated here that the nature of the group binding the fluorophore to the metal does not influence the photophysics.

The origin of the effect is geometrical in nature but is different from the celebrated odd–even effect well-known for thiols on gold[55–57] and is mainly caused by the large van der Waals interaction energy between pyrenes that competes with the chain−chain interaction energy to create structures with different local morphology.

Calculations and experiments suggest that the unexpected photophysical behavior is ultimately the result of the flexible chains that effectively modulate the fluorescence properties of the pyrene functionalized NPs via the modification of the tilt angle and the subsequent change of the interactions between metal and organic moiety. This promising mechanism has very recently been discussed by McGuiness *et al.*[58] and highlighted in a "perspective" contribution.[59] In our opinion, the appropriate selection of design motifs may be tuned to obtain a variety of desired fluorescence properties.

EXPERIMENTAL METHODS

All reagents were purchased from Sigma-Aldrich.

TOAB-stabilized gold nanoparticles were synthesized as already previously reported in ref 8.

Synthesis. The pyrene derivatives were obtained by mesylate **2** with nucleophilic substitution. Treating **2** with NaN_3 in DMF afforded the azide **3** that was reduced by $LiAlH_4$ to the corresponding amine **4**. Thioacetic pyrene ester **5** was prepared by nucleophilic displacement of the mesylate by $KSCOCH_3$,[60] and successive hydrolysis by KOH in acetone/water afforded the pyren-1-yl-butan-1-thiol **6**.

2′-(4-Pyren-1-yl-butylamine), 4. To a two bottom necked flask, 4-pyren-1-yl-butanol (0.4 g, 1.5 mmol), CH_2Cl_2 (1.5 mL), and *N,N′*-diisopropylethylamine (DIPEA; 0.46 mL, 2.6 mmol) were added under nitrogen; then the resulting solution was cooled to 0 °C. A solution of MsCl (0.155 mL, 2 mmol) in CH_2Cl_2 (1 mL) was added dropwise, then the mixture was stirred at 0 °C for 3 h. The mixture was quenched with ice/water, then was extracted with CH_2Cl_2 (2 × 5 mL). The collected organic phases were dried over Na_2SO_4 and concentrated under reduced pressure to give an oil purified by chromatography (eluant cyclohexane/ethyl acetate 1:1). The purified product **2**was dissolved in anhydrous DMF (9 mL); then NaN_3 (0.66 g, mmol) was added. The reaction mixture was stirred at RT for 24 h, then diluted with CH_2Cl_2 (20 mL) and quenched with water (5 mL). The organic phase was collected, washed with water (2 × 4 mL) and brine, then concentrated under reduced pressure to give an oil and purified by flash chromatography (eluant cyclohexane/acetate 9:1), giving 0.246 g yield of **3** in two steps, 55%. ^{1}H NMR ($CDCl_3$, 300 MHz) δ: 1.83–1.76 (m, 2H); 1.99–1.91 (m, 2H); 3.42–3.32 (m, 4H); 7.87 (d, 1H, *J* = 7.8 Hz); 8.00–7.96 (m, 3H); 8.20–8.11 (m, 4H); 8.27 (d, 1H, *J* = 9.3 Hz). ^{13}C NMR ($CDCl_3$, 75 MHz) δ: 136.1; 131.4; 130.9; 129.9; 128.6; 127.5; 127.4; 127.2; 126.7; 125.8; 125.1; 125.0; 124.9; 124.8; 124.7; 123.2; 51.36; 33.0; 28.9; 28.8.

The azide **3** (0.224 g, 0.75 mmol) was dissolved in THF (1.5 mL) and was added dropwise to a stirred solution of $LiAlH_4$ (0.071 g, 1.9 mmol) in THF (2 mL). The mixture was warmed to RT, then stirred for 3 h. The reaction was quenched with H_2O (0.070 mL), 15% solution of NaOH (0.070 mL), and then water again (0.14 mL). The mixture was stirred until white salts were formed, then filtered over a glass septum. The organic phase was acidified with 1 N HCL to pH = 1; the THF was evaporated under reduced pressure. The aqueous acid solution was extracted with ethyl acetate; then the aqueous phase was basified to pH = 11 with a NaOH, 5 M. The aqueous phase was extracted with diethyl ether (3 × 5 mL), and the collected organic phases were dried over Na_2SO_4 and evaporated under reduced pressure to give the 4-pyren-1-yl-butylamine as a pale yellow solid (0.150 mg, 69% yield). ^{1}H NMR ($CDCl_3$, 300 MHz) δ: 1.83–1.76 (m, 2H); 2.05–1.91 (m, 4H); 3.42–3.32 (m, 4H); 7.87 (d, 1H, *J* = 7.8 Hz); 8.00–7.96 (m, 3H); 8.20–8.11 (m, 4H); 8.27 (d, 1H, *J* = 9.3 Hz). ^{13}C NMR ($CDCl_3$, 75 MHz) δ: 136.8; 131.4; 130.9; 129.8; 128.6; 127.5; 127.2; 127.2; 126.5; 125.8; 125.1; 125.0; 124.8; 124.8; 124.6; 123.4; 42.16; 33.9; 33.4; 29.1.

Thioacetic Acid *S*-(4-Pyren-1-yl-butyl) Ester, 5. To a two bottom necked flask 4-pyren-1-yl-butanol (0.4 g, 1.5 mmol), CH_2Cl_2 (1.5 mL), and DIPEA (0.46 mL, 2.6 mmol) were added under nitrogen; then the resulting solution was cooled to 0 °C. A solution of MsCl (0.155 mL, 2 mmol) in CH_2Cl_2 (1 mL) was added dropwise; then the mixture was stirred at 0 °C for 3 h. The mixture was quenched with ice/water, then was extracted with CH_2Cl_2 (2 × 5 mL). The collected organic phases were dried over Na_2SO_4 and concentrated under reduced pressure to give an oil purified by chromatography (eluant cyclohexane/ethyl acetate 1:1). The purified mesylate **2** (0.42 g, 1.2 mmol) was dissolved in DMF (2 mL); then potassium thioacetate (0.3 g, 3 mmol) was added at room temperature. The mixture was stirred at RT for 4 h, diluted with diethyl ether (5 mL), then quenched with water (5 mL). The organic phase was separated, and the aqueous phase was extracted with diethyl ether (3 × 5 mL). The collected organic phases were reunited, dried over Na_2SO_4, and evaporated under reduce pressure to afford the crude product purified by chroma-

tography (cyclohexane/diethyl ether 8:2). The collected solid was suspended in diethyl ether, stirred for 10 min, then filtered over a glass septum. The pale yellow solid collected was washed with cold diethyl ether to yield thioacetic acid *S*-(4-pyren-1-yl-butyl) ester, **5**, 0.150 g, 45% yield. ^{1}H NMR ($CDCl_3$, 200 MHz) δ: 1.81–1.76 (m, 2H); 1.99–1.93 (m, 2H); 2.34 (s, 3H); 2.95 (t, 2H, J = 7.5 Hz); 3.35 (t, 2H, J = 7.5 Hz); 7.85 (d, 1H, J = 7.8 Hz); 8.20–8.25 (m, 8H). ^{13}C NMR ($CDCl_3$, 50 MHz) δ: 27.8; 28.8; 29.4; 30.6; 32.8; 123.16; 124.5; 124.6; 124.7; 124.8; 125.6; 126.4; 127.0; 127.1; 127.3; 128.4; 129.7; 130.7; 131.3; 134.4; 136.1; 195.7.

Pyren-1-yl-butan-1-thiol, 6. Solid KOH (0.2 g, 3.6 mmol) was dissolved in dry acetone (5 mL); then **5** (0.15 g, 0.49 mmol) and degassed water (0.6 mL) were added, and the reaction mixture was stirred under reflux conditions for 4 h. The reaction mixture was cooled to room temperature; then 1 N HCl was added until the pH was acid. The mixture was diluted with ether (10 mL) and stirred, and the phases were separated. The aqueous phase was extracted with ether (3 × 5 mL).The organic phases were reunited, dried over Na_2SO_4, and then evaporated under reduced pressure to give the crude mixture purified by chromatography (cyclohexane/diethyl ether 8:2) (0.60 g, 42% yield). ^{1}H NMR ($CDCl_3$, 200 MHz) δ: 1.85–1.77 (m, 2H); 2.08–1.99 (m, 2H); 2.64 (t, 2H, J = 7.5 Hz); 2.7 (s, 1H), 3.41 (t, 2H, J = 7.5 Hz); 7.90 (d, 2H, J = 7.5 Hz); 8.06–8.03 (m, 2H); 8.21–8.13 (m, 3H); 8.31 (d, 2H, J = 9 Hz). ^{13}C NMR ($CDCl_3$, 75 MHz) δ: 27.9; 29.4; 31.2; 33.1; 123.3; 124.6; 124.7; 124.8; 125.8; 126.5 (2C); 127.2; 127.5 (2C); 128.5; 129.7; 130.8; 131.4; 136.4 (2C).

Computational Procedures. The pyrene-terminated thiol chains were described by a standard force field.[61] Gold was described by an embedded atom model called "glue model".[62] Metal−organic interactions are the sum of long-distance and short-distance terms. The former are Coulomb interactions, with charges calculated as a function of the interatomic distances by the charge equilibration (QEq) scheme of Rappe and Goddard;[63] the latter are described by the short-range Born−Mayer potential, which tunes the long-distance one, accounts for higher order terms, and avoids nuclear fusion when charges interact attractively. Some examples of applications of this model are (i) the adsorption of alkanes and 1-alkenes on Au(111),[64]where the adsorption energies of short chains, up to C_{10}, were reproduced with an average error of less than 1 kcal mol^{-1} and the unexpected transition to disorder occurring for the deposition of alkyl chains between 18 and 26 carbon atoms was explained, (ii) the apparent symmetry breaking of a macrocyle on the Au surface,[65] (iii) the substitution kinetics of thiols on self-assembled monolayers,[41](iv) the existence of two surface reconstructions for C_{60} adsorbed on Au(110),[66] and (v) the mobility of DNA bases on Au(111).[67] The present model does not predefine the gold−organic connectivity, and molecules are able to slide on the surface. Some *ab initio* calculations of the total electronic energy were performed with the Gaussian03 suite of programs.[68]

Photophysical Experiments. The luminescence spectra were recorded with an Edinburgh FLS920 equipped with a photomultiplier Hamamatsu R928P. A PCS900 PC card was used for the time correlated single photon counting experiments. All the photophysical measurements were performed in aerated solutions.

The binding of the pyrene derivatives on the colloidal surfaces was monitored by fluorescence spectroscopy, as already reported for compound **C**.[42] In that case, in the same experimental conditions used here, there was a strong quenching of the fluorescence of **C** upon binding to the gold nanoparticles. In the fluorescence experiments, the concentration of the fluorophore was kept largely below the saturation level in order to minimize the fraction of unbound species and to avoid interfluorophore interaction.[42] For an easy interpretation of the fluorescence data, the commercial compound 1-methyl-pyrene, **D** (not shown), which does not bind to gold nanoparticles, was used as reference.

Acknowledgment. This work has been supported by MIUR through FIRB 2003-2004 LATEMAR (http://www.latemar.polito.it).

REFERENCES AND NOTES

1. Everts, M.; Saini, V.; Leddon, J. L.; Kok, R. J.; Stoff-Khalili, M.; Preuss, M. A.; Millican, C. L.; Perkins, G.; Brown, J. M.; Bagaria, H.; Nikles, D. E.; Johnson, D. T.; Zharov, V. P.; Curiel, D. T. Covalently Linked Au Nanoparticles to a Viral Vector: Potential for Combined Photothermal and Gene Cancer Therapy. *Nano Lett.* **2006**, *6*, 587–591.
2. Willner, B.; Katz, E.; Willner, I. Electrical Contacting of Redox Proteins by Nanotechnological Means. *Curr. Opin. Biotechnol.* **2006**, *17*, 589–596.
3. Lévy, R. Peptide-Capped Gold Nanoparticles: Towards Artificial Proteins. *ChemBioChem* **2006**, *7*, 1141–1145.
4. Templeton, A. C.; Welfing, W. P.; Murray, R. W. Monolayer Protected Cluster Molecules. *Acc. Chem. Res.* **2000**, *33*, 27–36.
5. Kamat, P. V. Photophysical, Photochemical and Photocatalytic Aspects of Metal Nanoparticles. *J. Phys. Chem. B* **2002**, *106*, 7729–7744.
6. Thomas, K. G.; Kamat, P. V. Chromophore-Functionalized Gold Nanoparticles. *Acc. Chem. Res.* **2003**, *36*, 888–898.
7. Shenhar, R.; Rotello, V. M. Nanoparticles: Scaffolds and Building Blocks. *Acc. Chem. Res.* **2003**, *36*, 549–561l.
8. Daniel, M. C.; Astruc, D. Gold Nanoparticles: Assembly, Supramolecular Chemistry, Quantum-Size-Related Properties, and Applications toward Biology, Catalysis, and Nanotechnology. *Chem. Rev.* **2004**, *104*, 293–346.
9. Drechsler, U.; Erdogan, B.; Rotello, V. M. Nanoparticles: Scaffolds for Molecular Recognition. *Chem.—Eur. J.* **2004**, *10*, 5570–5579.
10. Eustis, S.; El-Sayed, M. A. Why Gold Nanoparticles Are More Precious than Pretty Gold: Noble Metal Surface Plasmon Resonance and Its Enhancement of the Radiative and Nonradiative Properties of Nanocrystals of Different Shapes. *Chem. Soc. Rev.* **2006**, *35*, 209–217.
11. Lee, D.; Donkers, R. L.; Wang, G.; Harper, A. S.; Murray, R. W. Electrochemistry and Optical Absorbance and Luminescence of Molecule-Like Au-38 Nanoparticles. *J. Am. Chem. Soc.* **2004**, *126*, 6193–6199.
12. Guo, R.; Murray, R. W. Substituent Effects on Redox Potentials and Optical Gap Energies of Molecule-Like Au-38(SPhX)(24) Nanoparticles. *J. Am. Chem. Soc.* **2005**, *127*, 12140–12143.
13. Wang, G.; Huang, T.; Murray, R. W.; Menard, L.; Nuzzo, R. G. Near-IR Luminescence of Monolayer-Protected Metal Clusters. *J. Am. Chem. Soc.* **2005**, *127*, 812–813.
14. Dulkeith, E.; Niedereichholz, T.; Klar, T. A.; Feldmann, J. Plasmon Emission in Photoexcited Gold Nanoparticles. *Phys. Rev. B* **2004**, *70*, 205424-1–205424-4.
15. Wang, G.; Guo, R.; Kalyuzhny, G.; Choi, J.-P.; Murray, R. W. NIR Luminescence Intensities Increase Linearly with Proportion of Polar Thiolate Ligands in Protecting Monolayers of Au-38 and Au-140 Quantum Dots. *J. Phys. Chem. B* **2006**, *110*, 20282–20289.
16. Cheng, P. P. H.; Silvester, D.; Wang, G.; Kalyuzhny, G.; Douglas, A.; Murray, R. W. Dynamic and Static Quenching of Fluorescence by 1–4 nm Diameter Gold Monolayer-Protected Clusters. *J. Phys. Chem. B* **2006**, *110*, 4637–4644.
17. Montalti, M.; Zaccheroni, N.; Prodi, L.; O'Reilly, N.; James, S. L. Enhanced Sensitized NIR Luminescence from Gold Nanoparticles via Energy Transfer from Surface-Bound Fluorophores. *J. Am. Chem. Soc.* **2007**, *129*, 2418–2419.
18. Ruppin, R. Decay of an Excited Molecule Near a Small Metal Sphere. *J. Chem. Phys.* **1982**, *76*, 1681–1684.
19. Gersten, J.; Nitzan, A. Spectroscopic Properties of Molecules Interacting with Small Dielectric Particles. *J. Chem. Phys.* **1981**, *75*, 1139–1152.
20. Levi, S.; Mourran, A.; Spatz, J. P.; van Veggel, F. C. J. M.; Reinhoudt, D. N.; Möller, M. Fluorescence of Dyes Adsorbed on Highly Organized, Nanostructured Gold Surfaces. *Chem.—Eur. J.* **2002**, *8*, 3808–3814.
21. Dulkeith, E.; Morteani, A. C.; Niedereichholz, T.; Klar, T. A.; Feldmann, J.; Levi, S.; van Veggel, F. C. J. M.; Reinhoudt, D. N.; Möller, M.; Gittins, D. I. Fluorescence Quenching of Dye Molecules near Gold Nanoparticles: Radiative and Nonradiative Effects. *Phys. Rev. Lett.* **2002**, *89*, 203002.

22. Dulkeith, E.; Ringler, M.; Klar, T. A.; Feldmann, J.; Muñoz Javier, A.; Parak, W. J. Gold Nanoparticles Quench Fluorescence by Phase Induced Radiative Rate Suppression. *Nano Lett.* **2005**, *5*, 585–589.
23. Dubertret, B.; Calame, M.; Libchaber, A. J. Single-Mismatch Detection Using Gold-Quenched Fluorescent Oligonucleotides. *Nat. Biotechnol.* **2001**, *19*, 365–370.
24. Fan, C.; Wang, S.; Hong, J. W.; Bazan, G. C.; Plaxco, K. W.; Heeger, A. J. Beyond Superquenching: Hyper-Efficient Energy Transfer from Conjugated Polymers to Gold Nanoparticles. *Proc. Natl. Acad. Sci. U.S.A.* **2003**, *100*, 6297–6301.
25. Huang, C. C.; Chang, H. T. Selective Gold-Nanoparticle-Based "Turn-On" Fluorescent Sensors for Detection of Mercury(II) in Aqueous Solution. *Anal. Chem.* **2006**, *78*, 8332–8338.
26. Cannone, F.; Chirico, G.; Bizzarri, A. R.; Cannistraro, S. J. Quenching and Blinking of Fluorescence of a Single Dye Molecule Bound to Gold Nanoparticles. *J. Phys. Chem. B* **2006**, *110*, 16491–16498.
27. Wu, C. F.; Szymanski, C.; McNeill, J. Preparation and Encapsulation of Highly Fluorescent Conjugated Polymer Nanoparticles. *Langmuir* **2006**, *22*, 2956–2960.
28. Jennings, T. L.; Singh, M. P.; Strouse, G. F. Fluorescent Lifetime Quenching Near $d = 1.5$ nm Gold Nanoparticles: Probing NSET Validity. *J. Am. Chem. Soc.* **2006**, *128*, 5462–5467.
29. Jennings, T. L.; Schlatterer, J. C.; Singh, M. P.; Greenbaum, N. L.; Strouse, G. F. NSET Molecular Beacon Analysis of Hammerhead RNA Substrate Binding and Catalysis. *Nano Lett.* **2006**, *6*, 1318–1324.
30. Yun, C. S.; Javier, A.; Jennings, T.; Fisher, M.; Hira, S.; Peterson, S.; Hopkins, B.; Reich, N. O.; Strouse, G. F. Nanometal Surface Energy Transfer in Optical Rulers, Breaking the FRET Barrier. *J. Am. Chem. Soc.* **2005**, *127*, 3115–3119.
31. Anger, P.; Bharadwaj, P.; Novotny, L. Enhancement and Quenching of Single-Molecule Fluorescence. *Phys. Rev. Lett.* **2006**, *96*, 113002.
32. Tovmachenko, O. G.; Graf, C.; van den Heuvel, D. J.; van Blaaderen, A.; Gerritsen, H. C. Fluorescence Enhancement by Metal-Core/Silica-Shell Nanoparticles. *Adv. Mater.* **2006**, *18*, 91–95.
33. Tam, F.; Goodrich, G. P.; Johnson, B. R.; Halas, N. J. Plasmonic Enhancement of Molecular Fluorescence. *Nano Lett.* **2007**, *7*, 496–501.
34. Cheng, D. M.; Xu, Q. H. Separation Distance Dependent Fluorescence Enhancement of Fluorescein Isothiocyanate by Silver Nanoparticles. *Chem. Commun.* **2007**, 248–250.
35. Aslan, K.; Wu, M.; Lakowicz, J. R.; Geddes, C. D. Fluorescent Core-Shell Ag@SiO_2 Nanocomposites for Metal-Enhanced Fluorescence and Single Nanoparticle Sensing Platforms. *J. Am. Chem. Soc.* **2007**, *129*, 1524–1525.
36. Enderlein, J. Theoretical Study of Single Molecule Fluorescence in a Metallic Nanocavity. *Appl. Phys. Lett.* **2002**, *80*, 315–317.
37. Zhang, J.; Gryczynski, I.; Gryczynski, Z.; Lakowicz, J. R. Dye-Labeled Silver Nanoshell-Bright Particle. *J. Phys. Chem. B* **2006**, *110*, 8986–8991.
38. Thomas, K, G.; Kamat, P. V. Making Gold Nanoparticles Glow: Enhanced Emission from a Surface-Bound Fluoroprobe. *J. Am. Chem. Soc.* **2000**, *122*, 2655–2656.
39. Ipe, B. I.; Thomas, K. G.; Barazzouk, S.; Hotchandani, S.; Kamat, P. V. Photoinduced Charge Separation in a Fluorophore-Gold Nanoassembly. *J. Phys. Chem. B* **2002**, *106*, 18–21.
40. Kamat, P. V.; Barazzouk, S.; Hotchandani, S. Electrochemical Modulation of Fluorophore Emission on a Nanostructured Gold Film. *Angew. Chem., Int. Ed.* **2002**, *41*, 2764–2767.
41. Montalti, M.; Prodi, L.; Zaccheroni, N.; Baxter, R.; Teobaldi, G.; Zerbetto, F. Kinetics of Place-Exchange Reactions of Thiols on Gold Nanoparticles. *Langmuir* **2003**, *19*, 5172–5174.
42. Montalti, M.; Prodi, L.; Zaccheroni, N.; Battistini, G. Modulation of the Photophysical Properties of Gold Nanoparticles by Accurate Control of the Surface Coverage. *Langmuir* **2004**, *20*, 7884–7886.
43. Ipe, B. I.; Thomas, K. G. Investigations on Nanoparticle−Chromophore and Interchromophore Interactions in Pyrene-Capped Gold Nanoparticles. *J. Phys. Chem. B* **2004**, *108*, 13265–13272.
44. Wang, T. X.; Zhang, D. Q.; Xu, W.; Yang, J. L.; Han, R.; Zhu, D. B. Preparation, Characterization, and Photophysical Properties of Alkanethiols with Pyrene Units-Capped Gold Nanoparticles: Unusual Fluorescence Enhancement for the Aged Solutions of These Gold Nanoparticles. *Langmuir* **2002**, *18*, 1840–1848.
45. Ming, M.; Chen, M. M. Y.; Katz, A. Steady-State Fluorescence-Based Investigation of the Interaction Between Protected Thiols and Gold Nanoparticles. *Langmuir* **2002**, *18*, 2413–2420.
46. Boal, A. K.; Rotello, V. Radial Control of Recognition and Redox Processes with Multivalent Nanoparticle Hosts. *J. Am. Chem. Soc.* **2002**, *124*, 5019–5024.
47. Deng, J. P.; Wu, C. H.; Yang, C. H.; Mou, C. Y. Pyrene-Assisted Synthesis of Size-Controlled Gold Nanoparticles in Sodium Dodecyl Sulfate Micelles. *Langmuir* **2005**, *21*, 8947–8951.
48. Werts, M. H. V.; Zaim, H.; Blanchard-Desce, M. Excimer probe of the Binding of Alkyl Disulfides to Gold Nanoparticles and Subsequent Monolayer Dynamics. *Photochem. Photobiol. Sci.* **2004**, *3*, 29–32.
49. Shirdel, J.; Penzkofer, A.; Procházka, R.; Shen, Z.; Strauss, J.; Daub, J. Absorption and Emission Spectroscopic Characterisation of a Pyrene-Flavin Dyad. *Chem. Phys.* **2007**, *331*, 427–437.
50. Montalti, M.; Credi, A.; Prodi, L.; Gandolfi, M. T. *Handbook of Photochemistry*; CRC Press, Boca Raton, FL, 2006.
51. Credi, A.; Prodi, L. From Observed to Corrected Luminescence Intensity of Solution Systems: An Easy-to-Apply Correction Method for Standard Spectrofluorimeters. *Spectrochim. Acta, Part A* **1998**, *54*, 159–170.
52. Franzen, S.; Folmer, J. C. W.; Glomm, W. R.; O'Neal, R. Optical Properties of Dye Molecules Adsorbed on Single Gold and Silver Nanoparticles. *J. Phys. Chem. A* **2002**, *106*, 6533–6540.
53. von Lilienfeld, O. A.; Andrienko, D. Coarse-Grained Interaction Potentials for Polyaromatic Hydrocarbons. *J. Chem. Phys.* **2006**, *124*, 054307.
54. Arfaoui, I.; Bermudez, V.; Bottari, G.; De Nadai, C.; Jalkanen, J.-P.; Kajzar, F.; Leigh, D. A.; Lubomska, M.; Mendoza, S. M.; Niziol, J.; Rudolf, P.; Zerbetto, F. Surface Enhanced Second Harmonic Generation from Macrocycle, Catenane, and Rotaxane Thin Films: Experiments and Theory. *J. Phys. Chem. B* **2006**, *110*, 7648–7652.
55. Tao, F.; Bernasek, S. L. Understanding Odd-Even Effects in Organic Self-Assembled Monolayers. *Chem. Rev.* **2007**, *107*, 1408–1453.
56. Stoliar, P.; Kshirsagar, R.; Massi, M.; Annibale, P.; Albonetti, C.; de Leeuw, D. M.; Biscarini, F. Charge Injection Across Self-Assembly Monolayers in Organic Field-Effect Transistors: Odd-Even Effects. *J. Am. Chem. Soc.* **2007**, *129*, 6477–6484.
57. Love, J. C.; Estroff, L. A.; Kriebel, J. K.; Nuzzo, R. G.; Whitesides, G. M. Self-Assembled Monolayers of Thiolates on Metals as a Form of Nanotechnology. *Chem. Rev.* **2005**, *105*, 1103–1170.
58. McGuiness, C. L.; Blasini, D.; Masejewski, J. P.; Uppili, S.; Cabarcos, O. M.; Smilgies, D.; Allara, D. L. Molecular Self-Assembly at Bare Semiconductor Surfaces: Characterization of a Homologous Series of n-Alkanethiolate Monolayers on GaAs(001). *ACS Nano* **2007**, *1*, 30–49.
59. Bent, S. F. Heads or Tails: Which Is More Important in Molecular Self-Assembly. *ACS Nano* **2007**, *1*, 10–12.

60. Nakamura, F.; Hara, M. Hybridization of Polynucleotides Using Self-Assembled Monolayer Containing Pyrenyl Groups. *Mol. Cryst. Liq. Cryst.* **2002**, *377*, 57–60.
61. Allinger, N. L.; Yuh, Y. H.; Lii, J.-H. Molecular Mechanics. The MM3 Force Field for Hydrocarbons. 1. *J. Am. Chem. Soc.* **1989**, *111*, 8551–8566.
62. Ercolessi, F.; Parrinello, M.; Tosatti, E. Simulation of Gold in the Glue Model. *Philos. Mag. A* **1988**, *58*, 213–226.
63. Rappe, A. K.; Goddard, W. A., III. Charge Equilibration for Molecular Dynamics Simulations. *J. Phys. Chem.* **1991**, *95*, 3358–3363.
64. Baxter, R. J.; Teobaldi, G.; Zerbetto, F. Modeling the Adsorption of Alkanes on an Au(111) Surface. *Langmuir* **2003**, *19*, 7335–7340.
65. Whelan, C. M.; Cecchet, F.; Baxter, R.; Zerbetto, F.; Clarkson, G. J.; Leigh, D. A.; Rudolf, P. Adsorption of a Benzylic Amide Macrocycle on a Solid Substrate: XPS and HREELS Characterization of Thin Films Grown on Au(111). *J. Phys. Chem. B* **2002**, *106*, 8739–8746.
66. Baxter, R. J.; Rudolf, P.; Teobaldi, G.; Zerbetto, F. Modelling of the Adsorption of C-60 on the Au(110) Surface. *ChemPhysChem* **2004**, *5*, 245–248.
67. Rapino, S.; Zerbetto, F. Modeling the Stability and the Motion of DNA Nucleobases on the Gold Surface. *Langmuir* **2005**, *21*, 2512–2518.
68. Frisch, M. J.; Trucks, G. W.; Schlegel, H. B.; Scuseria, G. E.; Robb, M. A.; Cheeseman, J. R.; Montgomery, J. A., Jr.; Vreven, T.; Kudin, K. N.; Burant, J. C.; Millam, J. M.; Iyengar, S. S.; Tomasi, J.; Barone, V.; Mennucci, B.; Cossi, M.; Scalmani, G.; Rega, N.; Petersson, G. A.; Nakatsuji, H.; Hada, M.; Ehara, M.; Toyota, K.; Fukuda, R.; Hasegawa, J.; Ishida, M.; Nakajima, T.; Honda, Y.; Kitao, O.; Nakai, H.; Klene, M.; Li, X.; Knox, J. E.; Hratchian, H. P.; Cross, J. B.; Bakken, V.; Adamo, C.; Jaramillo, J.; Gomperts, R.; Stratmann, R. E.; Yazyev, O.; Austin, A. J.; Cammi, R.; Pomelli, C.; Ochterski, J. W.; Ayala, P. Y.; Morokuma, K.; Voth, G. A.; Salvador, P.; Dannenberg, J. J.; Zakrzewski, V. G.; Dapprich, S.; Daniels, A. D.; Strain, M. C.; Farkas, O.; Malick, D. K.; Rabuck, A. D.; Raghavachari, K.; Foresman, J. B.; Ortiz, J. V.; Cui, Q.; Baboul, A. G.; Clifford, S.; Cioslowski, J.; Stefanov, B. B.; Liu, G.; Liashenko, A.; Piskorz, P.; Komaromi, I.; Martin, R. L.; Fox, D. J.; Keith, T.; Al-Laham, M. A.; Peng, C. Y.; Nanayakkara, A.; Challacombe, M.; Gill, P. M. W.; Johnson, B.; Chen, W.; Wong, M. W.; Gonzalez, C.; Pople, J. A. *Gaussian 03*, revision C.02 Gaussian Inc.: Wallingford, CT, 2004.